Archival Report

Biological Psychiatry: CNNI

Abnormal Prefrontal Development in Pediatric Posttraumatic Stress Disorder: A Longitudinal Structural and Functional Magnetic Resonance Imaging Study

Sara A. Heyn, Taylor J. Keding, Marisa C. Ross, Josh M. Cisler, Jeanette A. Mumford, and Ryan J. Herringa

ABSTRACT

BACKGROUND: Prior studies of pediatric posttraumatic stress disorder (PTSD) have reported cross-sectional and age-related structural and functional brain abnormalities in networks associated with cognitive, affective, and self-referential processing. However, no reported studies have comprehensively examined longitudinal gray matter development and its intrinsic functional correlates in pediatric PTSD.

METHODS: Twenty-seven youths with PTSD and 21 nontraumatized typically developing (TD) youths were assessed at baseline and 1-year follow-up. At each visit, youths underwent structural magnetic resonance imaging and resting-state functional magnetic resonance imaging. Regions with volumetric abnormalities in whole-brain structural analyses were identified and used as seeds in exploratory intrinsic connectivity analyses.

RESULTS: Youths with PTSD exhibited sustained reductions in gray matter volume (GMV) in right ventromedial prefrontal cortex (PFC) and bilateral ventrolateral PFC. Group-by-time analyses revealed aberrant longitudinal development in dorsolateral PFC, where typically developing youths exhibited normative decreases in GMV between baseline and follow-up, and youths with PTSD showed increases in GMV. Using these regions as seeds, patients with PTSD exhibited atypical longitudinal decreases in intrinsic PFC–amygdala and PFC–hippocampus connectivity, in contrast to increases in typically developing youths. Specifically, youths with PTSD showed decreasing ventromedial PFC–amygdala connectivity as well as decreasing ventrolateral PFC–hippocampus connectivity over time. Notably, volumetric abnormalities in ventromedial PFC and ventrolateral PFC were predictive of symptom severity.

CONCLUSIONS: These findings represent novel longitudinal volumetric and connectivity changes in pediatric PTSD. Atypical prefrontal GMV and prefrontal-amygdala/hippocampus development may underlie persistence of PTSD in youths and could serve as future therapeutic targets.

Keywords: Childhood trauma, Functional magnetic resonance imaging, Neurodevelopment, Pediatric, Posttraumatic stress disorder, Structural magnetic resonance imaging

https://doi.org/10.1016/j.bpsc.2018.07.013

Pediatric posttraumatic stress disorder (PTSD) is classically characterized by re-experiencing, avoidance, and hyperarousal symptoms associated with childhood trauma exposure as well as changes in negative affect and cognition (1). PTSD is common in youths, with a lifetime prevalence of 4.7% and a point prevalence of 1.6% (2). Recent neuroimaging studies of pediatric PTSD suggest a pattern of neural abnormalities that are not simply a recapitulation of adult PTSD, but rather interact with dynamic structural and functional brain changes occurring in development. However, little is known about neural mechanisms underlying the maintenance of and recovery from PTSD over the course of development. Neurodevelopmental abnormalities in gray matter volume (GMV) and resting-state functional connectivity (RSFC) together may help to illuminate the pathway of PTSD progression across childhood. However, to date, no reported studies have longitudinally investigated pediatric PTSD across these domains.

Cross-sectional studies of pediatric PTSD point to abnormal structure and function in prefrontal-amygdala/hippocampus circuitry implicated in cognitive-emotional control and threat extinction (3). Two recent studies, including our own, showed that youths with PTSD have decreased GMV in the ventromedial prefrontal cortex (vmPFC) relative to nontraumatized typically developing (TD) youths (4) and trauma-exposed comparison youths (5). Structural abnormalities in the amygdala and hippocampus have been more variable. Using both region of interest (ROI) and

SEE COMMENTARY ON PAGE 103

ISSN: 2451-9022

voxelwise approaches, youths with PTSD were shown to have no differences in amygdalar or hippocampal GMV relative to TD youths (4–7). However, trauma-exposed comparison youths appear to have increased amygdalar and hippocampal GMV relative to youths with PTSD and TD youths, suggesting possible correlates of trauma resilience. Given reports of reduced hippocampal GMV in adult PTSD (8), the lack of deficits in pediatric PTSD may represent a delayed developmental effect in the hippocampus. Consistent with this notion, we found that youths with PTSD show decreased hippocampal volume with (cross-sectional) age, in contrast to increased volume with age in TD youths (4). Together, these findings suggest that reduced vmPFC volume and disrupted hippocampal development in youths with PTSD may contribute to deficits in cognitive-emotional control and threat extinction as youths age. To date, only pilot studies have longitudinally examined structural brain development in pediatric PTSD relative to comparison youths using ROI-based approaches (9,10). Larger studies of whole-brain morphometry are important to determine whether structural abnormalities persist and whether additional prefrontal changes may contribute to symptom persistence or recovery.

Functional magnetic resonance imaging (fMRI) studies of pediatric PTSD also suggest abnormal communication between medial prefrontal regions and the amygdala and hippocampus that may underlie illness expression. In emotion processing tasks, we have shown that youths with PTSD demonstrate decreased amygdala–medial PFC (mPFC) coupling to aversive stimuli (11–13) as well as decreased amygdala-vmPFC coupling with age (11). To date, only one reported study examined intrinsic prefrontal coupling with the amygdala and hippocampus in pediatric PTSD, although it did not examine age-related effects. Youths with PTSD showed decreased coupling between the basolateral amygdala and mPFC but increased centromedial amygdala–orbitofrontal cortex coupling relative to TD youths (14). Overall, these studies suggest impaired amygdala-mPFC coupling in pediatric PTSD, which may further contribute to deficits in cognitive-emotional control as youths age. However, it remains unclear how structural brain abnormalities relate to intrinsic communication or whether longitudinal changes in these circuits may contribute to symptom development in affected youths.

In this study, we provide the first whole-brain, longitudinal assessment of neurodevelopment in youths with PTSD using multimodal imaging. We first investigated structural morphometry, with the prediction that youths with PTSD would have persistent reductions in vmPFC volume and declining hippocampal volume over time. In exploratory analyses, we then seeded prefrontal regions that exhibited sustained or longitudinal GMV changes to investigate how structural abnormalities relate to RSFC with the amygdala/hippocampus complex. Based on our previous work, we hypothesized declining medial prefrontal-amygdala/hippocampus connectivity over time, which in turn would correlate with symptom severity.

METHODS AND MATERIALS

Participants

Participants included 36 medication-free (at baseline) youths with PTSD and 21 nontraumatized TD youths between the ages of 8 and 18 recruited from local mental health facilities and the general community, respectively. Exclusion criteria for youths with PTSD at study entry included IQ <70; history of psychotic disorder, bipolar disorder, or obsessive-compulsive disorder; active suicidality; recent (past 4 weeks) substance abuse or dependence; unstable medical condition; recent use of psychotropic medication (past 4 weeks, 6 weeks for fluoxetine); MRI contraindication; and pregnancy in female adolescents. No participants were taken off any psychotropic medication for the purposes of this study. Parental consent and youth assent were obtained for all participants, and all procedures used were approved by the University of Wisconsin Health Sciences Institutional Review Board. The majority of both groups attended both a baseline and a follow-up visit, resulting in 27 youths with PTSD and 21 TD youths in the final analyses.

All youths were assessed with structured trauma and psychiatric interviews with the Kiddie Schedule for Affective Disorders and Schizophrenia (15) at both time points. A PTSD diagnosis was determined using modified DSM-IV criteria (16) through a combination of the Kiddie Schedule for Affective Disorders and Schizophrenia and the Clinician-Administered PTSD Scale for Children and Adolescents (17). IQ scores for all youths were estimated using the Full-Scale IQ-2 component of the Wechsler Abbreviated Scale of Intelligence (18). One youth with PTSD was not able complete the full baseline IQ testing owing to fatigue. All youths completed the following additional assessments: Mood and Feelings Questionnaire (MFQ) (19), Screen for Child Anxiety Related Emotional Disorders (20), and Stressful Life Events Schedule Adolescent Self-Report (21). Youths with PTSD also completed the UCLA Child/Adolescent PTSD Reaction Index (PTSD-RI) (22). Further details regarding participant recruitment and assessment have been previously described (4,11,13).

Voxel-Based Morphometry

Structural MRI Acquisition and Preprocessing. Before both the baseline scan and the follow-up scan, youths completed two mock scanning sessions to accommodate them to the scanning environment and optimize data yield. MRI was performed using a Discovery MR750 3.0T scanner (GE Healthcare, Chicago, IL) with an eight-channel radiofrequency head coil at the University of Wisconsin Department of Psychiatry. Three-dimensional axial high-resolution T1 images were acquired with the following parameters: echo time = 3.18 ms, repetition time = 8.16 ms, inversion time = 450 ms, flip angle = 12°, field of view = 25.6 cm, slice thickness = 1.0 mm, 156 slices, and image matrix 256 × 256 that covered the entire brain. For whole-brain voxel-based morphometry (VBM), preprocessing was performed using the Computational Anatomy (CAT12) toolbox (http://dbm.neuro.uni-jena.de/cat/) in SPM12 (Wellcome Department of Imaging Neuroscience, London, United Kingdom) in MATLAB 8.3 (The MathWorks, Inc., Natick, MA). T1-weighted images were first processed using longitudinal segmentation, a rigid within-subject realignment, and one spatial normalization to all time points using default parameters in CAT12. Modulation and normalization of images included both affine and nonlinear registration. After preprocessing of structural images, the covariance structure of all

gray matter images was checked for homogeneity with all other images. Final voxel resolution was 1.5 × 1.5 × 1.5 mm.

Of the total sample, 22 youths with PTSD and 20 TD youths were included in final VBM analyses. One youth with PTSD was excluded owing to covariance being more than 2 SD below the mean as a result of significant motion artifact on close inspection. Three additional participants (2 youths with PTSD and 1 TD youth) were not included because the follow-up visit occurred after VBM analysis.

Statistical Analyses. Analyses on demographic and clinical data were examined using a two-tailed unpaired *t* test, and categorical data were assessed using χ^2 tests. R version 3.3.0 (23) and RStudio (24) were used for these analyses. For longitudinal GMV analysis (PTSD vs. TD), a general linear mixed-effects model was used to compute a voxelwise map of the main effect of group and a group-by-time interaction term, adjusting for age at baseline, sex, total intracranial volume, and subject as a random effect. Model parameters were estimated using Analysis of Functional NeuroImages (AFNI) 3dLME (25). Whole-brain familywise error correction was performed using Monte Carlo simulation (3dClustSim, -acf option; AFNI). At an individual voxel threshold of $p = .005$, the whole-brain cluster threshold was 495 voxels, resulting in familywise error corrected $p < .05$.

Resting-State Functional Connectivity

fMRI Acquisition and Preprocessing. Resting-state functional data were collected at the same slice locations as the T1-weighted anatomical data. Resting-state fMRI was performed using an echo-planar imaging (EPI) pulse sequence with the following parameters: sagittal orientation, echo time = 22 ms, repetition time = 2150 ms, flip angle = 79°, slice thickness = 3 mm, gap = 0.5 mm, 41 slices, field of view = 224 mm, and matrix 64 × 64. The scan lasted 5 minutes 16 seconds (repetition time = 146). During this time, youths were instructed to stay awake and rest with their eyes open but not to think of anything in particular. All preprocessing, including longitudinal registration, of individual resting-state scans at both time points was carried out in AFNI (26). Preprocessing of individual scans included 1) deletion of the first three volumes, 2) statistical outlier detection and despiking of fMRI data, 3) slice-timing correction, 4) coregistration of T1 and EPI images and realignment of EPI volumes, 5) motion correction and spatial smoothing (6 mm full width at half maximum), 6) anatomy segmentation, and 7) nuisance regression (eroded white matter, cerebrospinal fluid, six motion parameters and their derivatives) and motion censoring in a single step. Volumes were motion censored using a threshold of 0.25 mm based on framewise displacement calculated using the Euclidean norm.

During longitudinal registration, the T1 anatomical images at each time point were aligned, and a transformation matrix was output. The inverse, square-root-transformed mean transformation matrix was calculated and applied to each of the T1 images. The mean of the resulting images was calculated and then normalized to the Montreal Neurological Institute template. The square-root-transformed mean transformation matrix was then applied to the raw EPI datasets, the residual datasets from the aforementioned nuisance regression (output of 3dREMLfit), and the whole-brain masks at each time point. An intersection mask combining each time point's aligned mask was applied to each residual dataset, resulting in an output with only voxels in common between the two time points. Following longitudinal registration, temporal filtering (0.01 Hz < frequency < 0.1 Hz) was applied to the time series of each voxel. Participants having 25% of volumes flagged by the motion censoring algorithm (in either the time 1 or the time 2 images) were excluded from the study. The average motion in all directions was calculated and compared across groups, with no differences in motion observed. Final voxel resolution was 2 × 2 × 2 mm.

Of the total sample, 22 youths with PTSD and 21 TD youths were included in the final RSFC analyses. Seven youths were excluded because of motion artifact (PTSD group, $n = 3$) or follow-up scans that occurred after the VBM analyses had been completed (PTSD group, $n = 3$; TD group, $n = 1$).

Statistical Analyses. An exploratory seed-based connectivity analysis was conducted using prefrontal regions identified in the VBM analyses: left and right ventrolateral PFC (vlPFC), vmPFC, and left dorsolateral PFC (dlPFC) (resampled to EPI grid space). Pearson product-moment correlation coefficients were calculated between the average time course of each seed and all other voxels in the brain, converted to *z* values using the Fisher *z* transform, and entered into a second-level random-effects analysis implemented in AFNI. We used a linear mixed-effects model incorporating random effects to assess connectivity estimates as a function of group and group by time, adjusting for age at baseline, sex, and subject as a random effect. We conducted analyses in the a priori search region of the amygdala/hippocampus complex, which was created in AFNI by combining the bilateral amygdala and hippocampus ROIs [derived from (27)] included in the Anatomical Automatic Labeling atlas (http://neuro.imm.dtu.dk/wiki/Automated_Anatomical_Labeling). While these subcortical analyses were performed to explore the structural abnormalities identified in the primary VBM analyses, whole-brain analyses have been included in the Supplement. Whole-brain familywise error correction across all five seed-based analyses was performed using Monte Carlo simulation (3dClustSim, -acf option; AFNI). At an individual voxel threshold of $p = .005$, the cluster threshold was 20 voxels for the amygdala/hippocampus mask and 699 voxels for the whole-brain analyses, resulting in familywise error corrected $p < .05$. Given the exploratory nature of the RSFC analyses, we did not apply additional multiple comparison correction across the separate seed-based analyses.

RESULTS

Participant Characteristics

Participant characteristics are shown in Tables 1 and 2. Across groups, the average interscan interval was 1.22 years (Supplemental Figure S1). There were no differences between groups for sex, age, Tanner stage, or length of time between scans ($p > .05$). There was a significant group difference in IQ, with modestly lower IQ in the PTSD group ($t_{44} = 2.53$, $p = .015$)

Table 1. Full Sample Participant Characteristics

	TD (n = 22, F = 17)		PTSD (n = 27, F = 18)		Group Comparison	
	Time 1	Time 2	Time 1	Time 2	t	p
Age, Years, Mean (SD)	13.92 (2.44)	15.17 (2.49)	14.01 (2.81)	15.51 (3.15)	0.35	.73
Age, Years, Range	10.34–17.99	11.47–19.31	8.07–17.99	9.17–23.4		
IQ, Average	110	111.14	102.23	100.89	3.08	.0028
Tanner	3.29	3.79	2.94	3.85	0.7	.49
MFQ	3.05	3.95	24.56	20.29	−7.21	< .0001
SCARED	9.2	8.5	34.67	26	−7.62	< .0001

Typically developing (TD) and posttraumatic stress disorder (PTSD) groups did not differ significantly in sex distribution, age, or Tanner stage. The TD group had significantly higher IQ scores, whereas the PTSD group had significantly higher Mood and Feelings Questionnaire (MFQ) and Screen for Child Anxiety Related Mood Disorders (SCARED) scores. MFQ and SCARED represent the youth report scores. F, female.

(Table 1). On average, PTSD symptom severity (as measured by the PTSD-RI score) decreased by 32% between the baseline scan and follow-up scan (t_{24} = 3.33, p = .003) (Table 2). Of the 27 youths with PTSD, 11 had taken psychiatric medication before baseline, and 11 took psychiatric medication between baseline and follow-up. At the follow-up scan, 14 of the 27 youths with PTSD still met criteria for a PTSD diagnosis. Finally, almost all youths with PTSD were diagnosed with a comorbid disorder at either baseline (n = 21) or follow-up (n = 17).

Table 2. Additional PTSD Characteristics

	PTSD (n = 27, F = 18)	
	Time 1	Time 2
CAPS-CA	72.38	49.34
PTSD-RI	49.67	35.67
Index Trauma (n)	Sexual abuse (8)	
	Physical abuse/neglect (0)	
	Witnessing violence (3)	
	Traumatic accident/death (11)	
Comorbid Diagnoses (n)	Generalized anxiety disorder (5)	Generalized anxiety disorder (4)
	MDD single episode (10)	MDD single episode (5)
	MDD recurrent (2)	MDD recurrent (0)
	ADHD inattentive type (4)	ADHD inattentive type (6)
	ADHD hyperactive type (1)	Social anxiety disorder (3)
	ADHD combined type (3)	Separation anxiety disorder (2)
	Social anxiety disorder (4)	NOS (1)
	Separation anxiety disorder (9)	Depressive disorder (1)
	NOS (3)	Polysubstance dependence (2)
	Depressive disorder (2)	Adjustment disorder with depressed moods (1)
		Oppositional defiant disorder (1)
Psychiatric Medication (n)	Alpha agonist (1)	Alpha agonist (4)
	SSRI (3)	SSRI (11)
	Stimulant (8)	Stimulant (8)
	Benzodiazepine (2)	Benzodiazepine (1)
	Antipsychotic (1)	Serotonin antagonist (4)
	Anxiolytic (1)	Antihistamine (4)
	Serotonin antagonist (1)	NRI (1)
	Antihistamine (2)	SNRI (1)
		Lithium (1)
		TCA (1)
		Anticonvulsant/antiepileptic (1)
		Anxiolytic (1)

The Clinician-Administered PTSD Scale Child and Adolescent version (CAPS-CA) score was not obtained for the first 5 participants with posttraumatic stress disorder (PTSD). PTSD Reaction Index (PTSD-RI) represents the youth report scores.

ADHD, attention-deficit/hyperactivity disorder; F, female; MDD, major depressive disorder; NOS, not otherwise specified; NRI, norepinephrine reuptake inhibitor; SNRI, serotonin and norepinephrine reuptake inhibitor; SSRI, selective serotonin reuptake inhibitor; TCA, tricyclic antidepressant.

Longitudinal VBM: Whole-Brain Analyses

Whole-brain VBM results are summarized in Table 3. In both groups, decreases in GMV were found across the entire cortex over time (Figure 1). Group main effects revealed sustained decreases in GMV in the right anterior vmPFC (Brodmann areas [BAs] 10, 11), bilateral vlPFC (BAs 45, 47), right precentral gyrus (BA 44), and posterior cingulate cortex (BA 31) in youths with PTSD (Figure 2). A significant group-by-time effect was observed in the left dlPFC (BA 9). GMV in the dlPFC decreased over time in TD youths, whereas youths with PTSD showed slightly increasing GMV over time (Figure 2). Separate multivariate regressions in youths with PTSD on the group main effects and six symptom domains (MFQ, Screen for Child Anxiety Related Emotional Disorders, PTSD-RI subscore B/C/D, and PTSD-RI total; covaried for age at baseline, sex, and total intracranial volume) revealed three significant symptom relationships. GMV in the left vlPFC is negatively predictive of depression symptoms (MFQ: $t_{38} = -2.24$, $p = .03$) (Figure 2), GMV in the vmPFC was negatively predictive of anxiety symptoms (SCARED: $t_{38} = -2.01$, $p = .05$) (Figure 2), and posterior cingulate cortex GMV was positively predictive of overall PTSD symptom severity (PTSD-RI total: $t_{38} = 2.192$, $p = .02$).

Resting-State Prefrontal Connectivity: Seed-Based Analyses

Among the sustained and developmental abnormalities identified in the VBM analyses, we were interested in interrogating the four prefrontal regions identified: bilateral vlPFC, vmPFC, and dlPFC. Here we report RSFC findings within our a priori amygdala/hippocampus search region, summarized in Table 4. In a significant group-by-time interaction, youths with PTSD exhibited aberrant longitudinal intrinsic functional connectivity between the vmPFC and left amygdala ([26, 8, −16]; k = 26; $Z = -3.79$). Specifically, TD youths showed increasing (more positive) connectivity over time, whereas youths with PTSD showed decreasing (more negative) connectivity over time (Figure 3). An additional significant group-by-time interaction revealed abnormal intrinsic connectivity between the left vlPFC and the left anterior hippocampus ([32, 12, −18]; k = 22; $Z = -3.95$). The dlPFC seed also showed a group-by-time interaction with the left anterior hippocampus at trend level ([34, 18, −24]; k = 17; $Z = -3.22$; $p = .07$). In both cases, TD youths showed increasing (more positive) connectivity over time, whereas youths with PTSD exhibited the opposite effect (Figure 3). Separate multivariate regressions in youths with PTSD on connectivity findings revealed symptom relationships only with dlPFC-hippocampus connectivity. Here, dlPFC-hippocampus coupling was inversely related to anxiety, depression, and PTSD severity (see Supplement).

Post Hoc Analyses

All remaining post hoc analyses are fully described in the Supplement and are briefly reviewed here. Across all morphometric and functional connectivity analyses, all group and group-by-time findings remained statistically significant or near significant when adjusting for other potential explanatory variable measures, including IQ, Tanner stage, trauma load, age at index trauma, previous use of any type of psychiatric medication, or history of psychotherapy. It is important to note that while the exploratory analyses above suggest that lack of significant abnormalities in hippocampal GMV was driven by interim selective serotonin reuptake inhibitor (SSRI) use, post hoc analyses on regions with significant structural abnormalities were not significantly influenced by psychiatric medication use. Finally, the perceived impact of stressful life events before baseline and between time points was not predictive of any of the structural or functional abnormalities identified.

DISCUSSION

To our knowledge, this is the first multimodal, longitudinal analysis of neurodevelopment in pediatric PTSD. We report novel findings, including sustained reductions and abnormal neurodevelopment in key prefrontal nodes in youths with PTSD compared with TD youths. Specifically, we have replicated reduced vmPFC GMV found in our previous cross-sectional analysis of the baseline cohort in this longitudinal analysis (4) as well as identifying additional regions in the vlPFC showing sustained GMV reductions. Furthermore, youths with PTSD exhibit abnormal increases in dlPFC volume in contrast to normative, widespread decreases elsewhere in the cortex. Notably, these prefrontal nodes with structural abnormalities also showed evidence of declining intrinsic connectivity with

Table 3. Summary of Structural MRI Longitudinal Analyses: Whole-Brain VBM

Contrast	Region	Laterality	BA	Peak Z	x	y	z	Cluster Voxels
TD > PTSD	vlPFC	R	45/47	3.27	−43.5	−43.5	−3	1653
	PCC	B	31	3.39	−1.5	75.5	36	1082
	Precentral gyrus	R	44	3.61	−60	−4.5	22.5	951
	vlPFC	L	45/47	3.38	45	−37.5	6	910
	vmPFC	R	10/11	3.57	−10.5	−64.5	−10.5	702
Group × Time	dlPFC	L	9	2.83	22.5	−27	43.5	649
PTSD > TD								

Clusters shown survived whole-brain cluster correction (corrected $p < .05$). Peak coordinates (x, y, z) are reported based on the Montreal Neurological Institute atlas in left, posterior, inferior orientation. All analyses included age at baseline, sex, and total intracranial volume as covariates.

B, bilateral; BA, Brodmann area; dlPFC, dorsolateral prefrontal cortex; L, left; MRI, magnetic resonance imaging; PCC, posterior cingulate cortex; PTSD, posttraumatic stress disorder; R, right; TD, typically developing; VBM, voxel-based morphometry; vlPFC, ventrolateral prefrontal cortex; vmPFC, ventromedial prefrontal cortex.

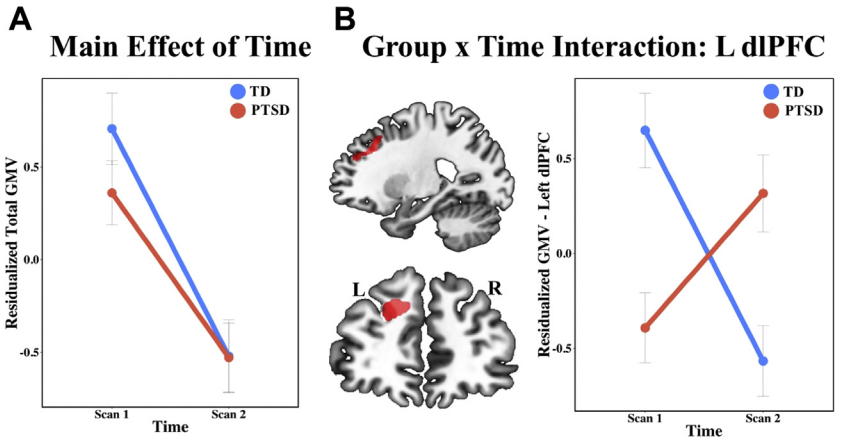

Figure 1. Longitudinal gray matter abnormalities and symptom correlations in youths with posttraumatic stress disorder (PTSD) (n = 22) compared to typically developing (TD) youths (n = 20). **(A)** Global decreases in gray matter volume (GMV) with time for both TD youths and youths with PTSD as shown by a main effect of scan, covaried for age at baseline, sex, total intracranial volume, and subject as a random effect (k = 133,285). **(B)** Group × time interaction, covaried for age at baseline, sex, total intracranial volume, and subject as a random effect, revealed that time positively predicted GMV in the left dorsolateral prefrontal cortex (dlPFC) in youths with PTSD but negatively predicted GMV in TD youth (k = 649; p = .05). L, left; R, right.

the amygdala/hippocampus complex over time in youths with PTSD in subsequent exploratory analyses. These results suggest that prefrontal structural abnormalities may reflect abnormal development of intrinsic prefrontal network function in youths with PTSD.

Our findings are highly consistent with existing circuit models of PTSD and psychopathology more broadly. Reduced vmPFC volume has now been demonstrated in both adult and pediatric PTSD, and the present findings suggest that this reflects a sustained pattern in pediatric PTSD. The vmPFC is notable for its role in the top-down modulation of amygdala responses and the inhibition of threat responses in both humans and rats (28,29). Consistent with this notion, we also observed reductions in vmPFC-amygdala connectivity over time in youth with PTSD. This stands in contrast to increased coupling over time in our TD youths as well as documented cross-sectional age-related increases in vmPFC-amygdala intrinsic connectivity in TD youths (30). Furthermore, these findings are consistent with reduced basolateral amygdala–mPFC intrinsic connectivity previously reported in adolescent PTSD (14). Taken together, these findings suggest that vmPFC structural abnormalities and reduced vmPFC-amygdala

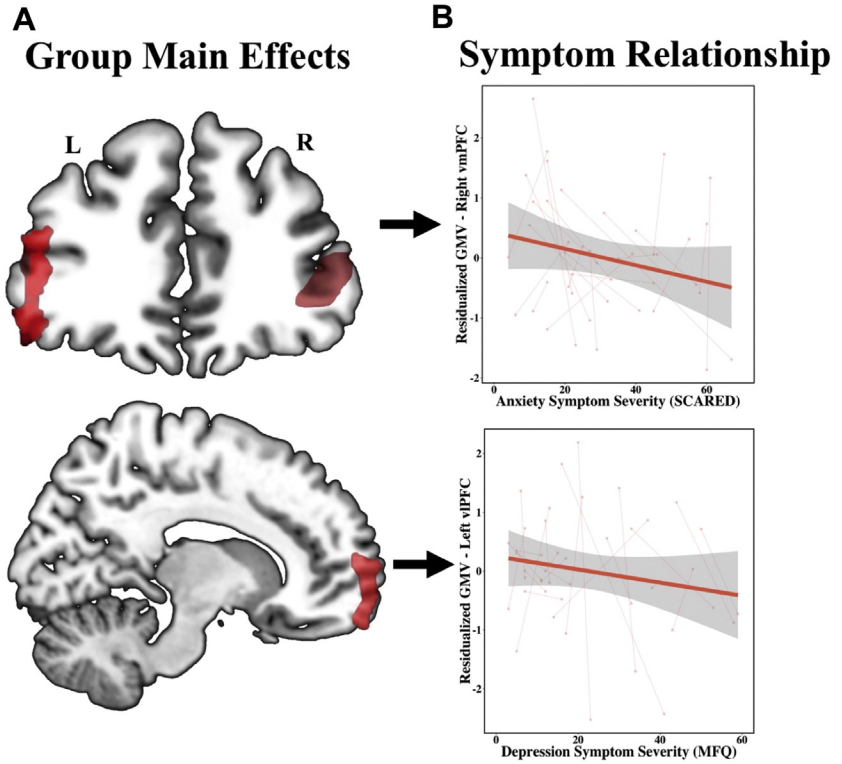

Figure 2. Gray matter abnormalities and symptom correlations in youths with posttraumatic stress disorder (PTSD) (n = 22) compared with typically developing youths (n = 20). **(A)** Reduced gray matter volume (GMV) in the bilateral ventrolateral prefrontal cortex (vlPFC) and right ventromedial PFC (vmPFC) in youths with PTSD compared with typically developing youths, covaried for age at baseline, sex, total intracranial volume, and subject as a random effect. **(B)** Depression symptoms of PTSD, as measured by the Mood and Feelings Questionnaire (MFQ), are inversely correlated with bilateral vlPFC GMV, and anxiety symptoms, as measured by the Screen for Child Anxiety Related Emotional Disorders (SCARED), are inversely correlated with vmPFC GMV, covaried for age at baseline, sex, total intracranial volume, subject as a random effect, and the four alternative symptom scores (PTSD Reaction Index cluster B, C, D, and MFQ/SCARED). Scatterplot shows extracted cluster data in relation to depression symptom severity. L, left; R, right.

Table 4. Summary of Seed-Based RSFC Longitudinal Analyses

Contrast	Mask	Seed	Target	Laterality	Peak Z	k	x	y	z
Group × Time	Limbic	R vmPFC	Amygdala	L	−3.79	26	26	8	−16
	Limbic	L vlPFC	Hippocampus	L	−3.95	22	32	12	−18
	Limbic[a]	L dlPFC[a]	Hippocampus[a]	L[a]	−3.22[a]	17[a]	34[a]	18[a]	−24[a]
	Limbic	PCC	Amygdala	L	−3.9	16	28	10	−16

Clusters shown survived cluster correction (corrected $p < .05$) within the limbic mask. Peak coordinates (x, y, z) are reported based on the Montreal Neurological Institute atlas in left, posterior, inferior orientation. All analyses included age at baseline, sex, and subject as a random effect.

dlPFC, dorsolateral prefrontal cortex; L, left; PCC, posterior cingulate cortex; R, right; RSFC, resting-state functional connectivity; vlPFC, ventrolateral prefrontal cortex; vmPFC, ventromedial prefrontal cortex.

[a]Trending effect following correction ($p < .08$).

coupling over time may contribute to threat extinction deficits in pediatric PTSD, which may worsen with age.

Next, we also found evidence of volumetric abnormalities in the vlPFC and dlPFC, which represent novel findings in pediatric PTSD. Youths with PTSD exhibited sustained reductions in GMV in bilateral vlPFC as well as abnormal increases in GMV in the dlPFC. The vlPFC and dlPFC have both been heavily implicated in emotion regulation processes (31,32). In particular, the vlPFC is involved in selection and inhibition of cognitive appraisals (31,33), whereas the dlPFC has consistently been associated with explicit emotion regulation through cognitive reappraisal (31,34,35). Interestingly, both of these nodes showed evidence of reduced intrinsic connectivity over time with the anterior hippocampus, in contrast to increases in TD youths. The hippocampus is known to be involved in the contextual regulation of emotion, including gating of conditioned threat responses. However, the anterior hippocampus, which has extensive amygdala projections, is also preferentially involved in unconditioned threat responses. While neither VBM nor RSFC analyses are inherently able to provide information regarding the functional significance of regions identified as having group or longitudinal abnormalities, we speculate based on the prior literature that our observed decreases in vlPFC/dlPFC-hippocampus connectivity in youths with PTSD may reflect loss of inhibitory control of unconditioned threat responses over time and could conceivably contribute to increasing threat acquisition and impaired threat extinction in pediatric PTSD. This notion is further supported by the symptom relationships identified between dlPFC-hippocampus connectivity and anxiety, depression, and PTSD symptom severity (Supplemental Figure S2). However, future studies specifically incorporating threat learning and emotion regulation tasks will clearly be needed to address these possibilities.

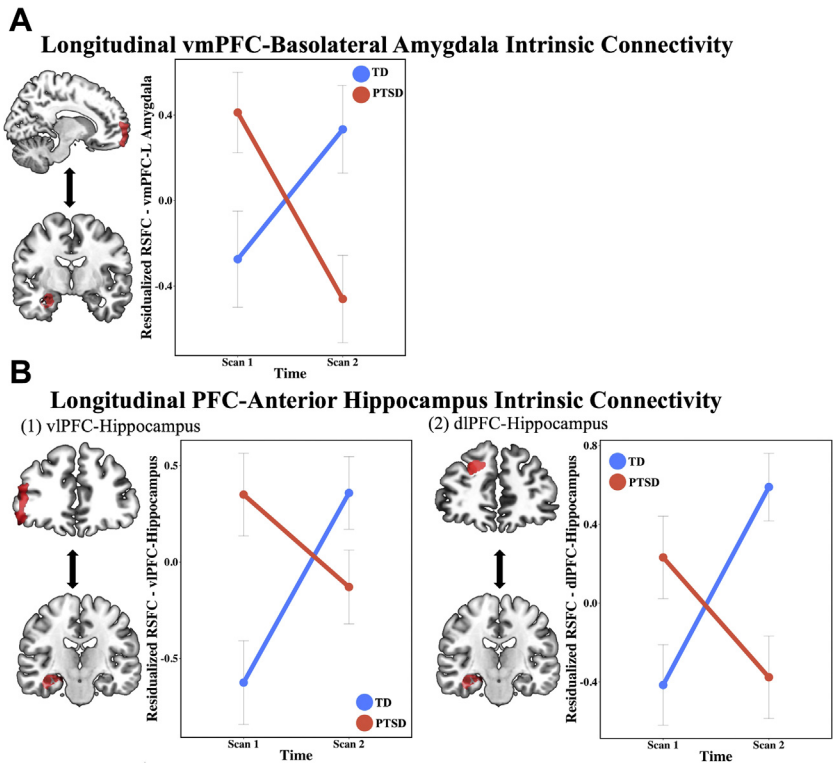

Figure 3. Longitudinal prefrontal intrinsic connectivity abnormalities and symptom correlations in youths with posttraumatic stress disorder (PTSD) (n = 22) compared with typically developing (TD) youths (n = 20). **(A)** Longitudinal changes in resting-state connectivity using the right ventromedial prefrontal cortex (vmPFC) cluster identified in voxel-based morphometry analyses as a seed region. A significant group × time interaction, covaried for age at baseline, sex, and subject as a random effect, revealed that intrinsic connectivity between the vmPFC and right basolateral amygdala exhibited longitudinal increases in TD youths and longitudinal decreases in youths with PTSD. **(B)** (Panel 1) Longitudinal changes in resting-state connectivity using the left ventrolateral PFC (vlPFC) cluster identified in the voxel-based morphometry analyses as a seed region. A significant group × time interaction, covaried for age at baseline, sex, and subject as a random effect, revealed that intrinsic connectivity between the vlPFC and the anterior hippocampus exhibited longitudinal increases in TD youths and longitudinal decreases in youths with PTSD. (Panel 2) A similar trending group × time interaction with the anterior hippocampus was identified using the dorsolateral PFC (dlPFC) cluster identified in voxel-based morphometry analyses as a seed region. For graphing and post hoc analyses, the average connectivity estimate was extracted for significant clusters. RSFC, resting-state functional connectivity.

Surprisingly, we were unable to detect abnormal volumetric change in the hippocampus over a 1-year period in the youths with PTSD. Our prior study, albeit cross-sectional, found evidence of decreased right anterior hippocampal volume with age in youths with PTSD (2). Even with signal averaging across voxels over a hippocampal ROI, we were unable to detect an association between hippocampal volume and PTSD. Based on the ROI data, the estimated chance of type II error is $\beta = .28$. One possible explanation could be that medication exposure in youths with PTSD is masking these effects. Notably, SSRIs are known to increase hippocampal neurogenesis (36,37) and appear to increase hippocampal GMV in adults with PTSD (38,39). Intriguingly, an exploratory analysis revealed an interaction effect with SSRI use in the right anterior hippocampus. Youths with PTSD who had taken an SSRI between baseline and follow-up (n = 6) showed increased hippocampal GMV over time compared with youths with PTSD not exposed to SSRIs (n = 16) or TD youths (n = 20) (Supplemental Figure S2). These findings, although preliminary, suggest that SSRI use may counteract hippocampal volume decline in youths with PTSD. Further study in larger samples of youths in a randomized controlled treatment design is warranted to determine whether SSRI use is indeed capable of augmenting hippocampal volume in youths with PTSD. Similarly, future studies are warranted to determine whether current evidence-based therapies, such as trauma-focused cognitive behavioral therapy, are capable of correcting prefrontal volumetric deficits in pediatric PTSD and to what extent GMV and RSFC changes may mediate the effects of treatment. Notably, recent studies in adult PTSD (40–42) suggest that both psychotherapy and SSRI treatment may augment function in prefrontal regions (vlPFC, dlPFC) implicated in cognitive-emotional control.

Although this study has identified novel neurodevelopmental abnormalities in prefrontal-amygdala/hippocampus circuitry in pediatric PTSD, it is not without limitations. First, although we strove to appropriately match our groups and adjust for potentially confounding variables in post hoc analyses, we cannot rule out the possibility that these results could be accounted for by an unknown third variable. Second, youths were allowed to receive treatment as usual in the community. However, all participants were unmedicated at the time of the baseline scan, and all results remained significant after adjusting for medication and psychotherapy. Third, our sample is only moderate in size with a single follow-up scan. A replication and/or extension of our current study to multiple time points with a larger sample size is warranted. Finally, our cohort of recruited youths with PTSD were typically exposed to more than one trauma. Age and chronicity of trauma exposure are likely influential factors on prefrontal-amygdala/hippocampus development as well as other circuits (43). However, given our moderate sample size, we were not able to fully explore sensitive periods with regard to the neural abnormalities identified. Finally, to differentiate the effects specific to PTSD from the general effects of childhood trauma, future studies should include a trauma-exposed group.

In summary, our results provide the first longitudinal evidence of sustained and developmental structural and functional abnormalities in key prefrontal-amygdala/hippocampus circuits in pediatric PTSD. Notably, reduced volume and abnormal development in these prefrontal nodes was associated with declining functional connectivity over time with the amygdala/hippocampus complex, implicating these prefrontal circuits in the persistence of PTSD and its comorbidities in developing youth. Future studies are warranted to further explore the diagnostic specificity of these developmental patterns and test whether current evidence-based treatments are capable of restoring healthy neurodevelopment, or compensatory neurodevelopment, in youths with PTSD.

ACKNOWLEDGMENTS AND DISCLOSURES

This work was supported by the National Institute of Mental Health Career Development Award (Grant No. K08 MH100267 [to RJH]), American Academy of Child and Adolescent Psychiatry Junior Investigator Award (to RJH), National Alliance for Research on Schizophrenia and Depression Young Investigator Grant (to RJH), University of Wisconsin Institute for Clinical and Translational Research Translational Pilot Grant Award (National Institutes of Health National Center for Advancing Translational Sciences Grant No. UL1TR000427 [to RJH]), University of Wisconsin Institute of Clinical and Translational TL1 Training Award (Grant No. TL1TR000429 [to SAH]), and University of Wisconsin School of Medicine and Public Health. None of these funding sources had a direct effect on the design, analysis, or interpretation of the study results or in preparation of the manuscript.

This material is based upon work supported by the National Science Foundation Graduate Research Fellowship Program under Grant No. DGE-1747503 (to TJK). Any opinions, findings, and conclusions or recommendations expressed in this material are those of the author(s) and do not necessarily reflect the views of the National Science Foundation. Support was also provided by the Graduate School and the Office of the Vice Chancellor for Research and Graduate Education at the University of Wisconsin-Madison with funding from the Wisconsin Alumni Research Foundation.

We thank Rachael Meline and Shelby Weaver for their work in the recruitment and data collection for this study.

Data presented at the Society for Research in Child Development Biennial Meeting, April 6–8, 2017, Austin, Texas.

The authors report no biomedical financial interests or potential conflicts of interest.

ARTICLE INFORMATION

From the Neuroscience and Public Policy Program (SAH), Neuroscience Training Program (SAH, TJK, MCR, JMC, RJH), and Center for Healthy Minds (JAM), University of Wisconsin-Madison; and Department of Psychiatry (JMC, RJH), University of Wisconsin-Madison School of Medicine and Public Health, Madison, Wisconsin.

Address correspondence to Sara A. Heyn, M.S., J.D., BRAVE Youth Lab, Department of Psychiatry, University of Wisconsin-Madison, 6001 Research Park Boulevard, Room 1329, Madison, WI 53719; E-mail: sheyn@wisc.edu.

Received Mar 29, 2018; revised and accepted Jul 27, 2018.

Supplementary material cited in this article is available online at https://doi.org/10.1016/j.bpsc.2018.07.013.

REFERENCES

1. American Psychiatric Association (2013): Diagnostic and Statistical Manual of Mental Disorders, 5th ed. Washington, DC: American Psychiatric Association.
2. McLaughlin KA, Koenen KC, Hill ED, Petukhova M, Sampson NA, Zaslavsky AM, *et al.* (2013): Trauma exposure and posttraumatic stress disorder in a national sample of adolescents. J Am Acad Child Adolesc Psychiatry 52:815–830.e14.
3. Herringa RJ (2017): Trauma, PTSD, and the developing brain. Curr Psychiatry Rep 19:69.
4. Keding TJ, Herringa RJ (2015): Abnormal structure of fear circuitry in pediatric post-traumatic stress disorder. Neuropsychopharmacology 40:537–545.

5. Morey RA, Haswell CC, Hooper SR, De Bellis MD (2016): Amygdala, hippocampus, and ventral medial prefrontal cortex volumes differ in maltreated youth with and without chronic posttraumatic stress disorder. Neuropsychopharmacology 41:791–801.
6. Carrion VG, Weems CF, Eliez S, Patwardhan A, Brown W, Ray RD, *et al.* (2001): Attenuation of frontal asymmetry in pediatric posttraumatic stress disorder. Biol Psychiatry 50:943–951.
7. De Bellis MD, Keshavan MS, Shifflett H, Iyengar S, Beers SR, Hall J, *et al.* (2002): Brain structures in pediatric maltreatment-related posttraumatic stress disorder: A sociodemographically matched study. Biol Psychiatry 52:1066–1078.
8. Kuhn S, Gallinat J (2013): Gray matter correlates of posttraumatic stress disorder: A quantitative meta-analysis. Biol Psychiatry 73: 70–74.
9. De Bellis MD, Hall J, Boring AM, Frustaci K, Moritz G (2001): A pilot longitudinal study of hippocampal volumes in pediatric maltreatment-related posttraumatic stress disorder. Biol Psychiatry 50:305–309.
10. Carrion VG, Weems CF, Reiss AL (2007): Stress predicts brain changes in children: A pilot longitudinal study on youth stress, posttraumatic stress disorder, and the hippocampus. Pediatrics 119: 509–516.
11. Wolf RC, Herringa RJ (2016): Prefrontal-amygdala dysregulation to threat in pediatric posttraumatic stress disorder. Neuropsychopharmacology 41:822–831.
12. Cisler JM, Scott Steele J, Smitherman S, Lenow JK, Kilts CD (2013): Neural processing correlates of assaultive violence exposure and PTSD symptoms during implicit threat processing: A network-level analysis among adolescent girls. Psychiatry Res 214:238–246.
13. Keding TJ, Herringa RJ (2016): Paradoxical prefrontal-amygdala recruitment to angry and happy expressions in pediatric posttraumatic stress disorder. Neuropsychopharmacology 41:2903–2912.
14. Aghajani M, Veer IM, van Hoof MJ, Rombouts SA, van der Wee NJ, Vermeiren RR (2016): Abnormal functional architecture of amygdala-centered networks in adolescent posttraumatic stress disorder. Hum Brain Mapp 37:1120–1135.
15. Kaufman J, Birmaher B, Brent D, Rao U, Flynn C, Moreci P, *et al.* (1997): Schedule for Affective Disorders and Schizophrenia for School-Age Children-Present and Lifetime Version (K-SADS-PL): Initial reliability and validity data. J Am Acad Child Adolesc Psychiatry 36:980–988.
16. Cohen JA, Mannarino AP, Iyengar S (2011): Community treatment of posttraumatic stress disorder for children exposed to intimate partner violence: a randomized controlled trial. Arch Pediatr Adolesc Med 165:16–21.
17. Weathers FW, Keane TM, Davidson JR (2001): Clinician-administered PTSD scale: A review of the first ten years of research. Depress Anxiety 13:132–156.
18. Wechsler D (2011): Wechsler Abbreviated Scale of Intelligence–Second Edition Manual. Bloomington, MN: Pearson.
19. Costello EJ, Angold A (1988): Scales to assess child and adolescent depression: Checklists, screens, and nets. J Am Acad Child Adolesc Psychiatry 27:726–737.
20. Birmaher B, Khetarpal S, Brent D, Cully M, Balach L, Kaufman J, *et al.* (1997): The Screen for Child Anxiety Related Emotional Disorders (SCARED): Scale construction and psychometric characteristics. J Am Acad Child Adolesc Psychiatry 36:545–553.
21. Williamson DE, Birmaher B, Ryan ND, Shiffrin TP, Lusky JA, Protopapa J, *et al.* (2003): The stressful life events schedule for children and adolescents: Development and validation. Psychiatry Res 119:225–241.
22. Steinberg AM, Brymer MJ, Decker KB, Pynoos RS (2004): The University of California at Los Angeles Post-traumatic Stress Disorder Reaction Index. Curr Psychiatry Rep 6:96–100.
23. R Core Team (2013): R: A language and environment for statistical computing. Vienna, Austria: R Foundation for Statistical Computing. Available at: https://www.R-project.org.
24. RStudio Team (2015): RStudio: Integrated Development for R. Boston, MA: RStudio, Inc. Available at: http://www.rstudio.com/.
25. Chen G, Saad ZS, Britton JC, Pine DS, Cox RW (2013): Linear mixed-effects modeling approach to FMRI group analysis. Neuroimage 73:176–190.
26. Cox RW (1996): AFNI: Software for analysis and visualization of functional magnetic resonance neuroimages. Comput Biomed Res Int J 29:162–173.
27. Amunts K, Kedo O, Kindler M, Pieperhoff P, Mohlberg H, Shah NJ, *et al.* (2005): Cytoarchitectonic mapping of the human amygdala, hippocampal region and entorhinal cortex: intersubject variability and probability maps. Anat Embryol (Berl) 210:343–352.
28. Milad MR, Quirk GJ (2002): Neurons in medial prefrontal cortex signal memory for fear extinction. Nature 420:70–74.
29. Rougemont-Bücking A, Linnman C, Zeffiro TA, Zeidan MA, Lebron-Milad K, Rodriguez-Romaguera J, *et al.* (2011): Altered processing of contextual information during fear extinction in PTSD: An fMRI study. CNS Neurosci Ther 17:227–236.
30. Gabard-Durnam LJ, Flannery J, Goff B, Gee DG, Humphreys KL, Telzer E, *et al.* (2014): The development of human amygdala functional connectivity at rest from 4 to 23 years: A cross-sectional study. Neuroimage 95:193–207.
31. Buhle JT, Silvers JA, Wager TD, Lopez R, Onyemekwu C, Kober H, *et al.* (2014): Cognitive reappraisal of emotion: A meta-analysis of human neuroimaging studies. Cereb Cortex 24:2981–2990.
32. Wager TD, Davidson ML, Hughes BL, Lindquist MA, Ochsner KN (2008): Prefrontal-subcortical pathways mediating successful emotion regulation. Neuron 59:1037–1050.
33. Robbins TW (2007): Shifting and stopping: Fronto-striatal substrates, neurochemical modulation and clinical implications. Philos Trans R Soc Lond B Biol Sci 362:917–932.
34. Goldin PR, McRae K, Ramel W, Gross JJ (2008): The neural bases of emotion regulation: Reappraisal and suppression of negative emotion. Biol Psychiatry 63:577–586.
35. McRae K, Gross JJ, Weber J, Robertson ER, Sokol-Hessner P, Ray RD, *et al.* (2012): The development of emotion regulation: An fMRI study of cognitive reappraisal in children, adolescents and young adults. Soc Cogn Affect Neurosci 7:11–22.
36. Santarelli L, Saxe M, Gross C, Surget A, Battaglia F, Dulawa S, *et al.* (2003): Requirement of hippocampal neurogenesis for the behavioral effects of antidepressants. Science 301:805–809.
37. Powell TR, Murphy T, de Jong S, Lee SH, Tansey KE, Hodgson K, *et al.* (2017): The genome-wide expression effects of escitalopram and its relationship to neurogenesis, hippocampal volume, and antidepressant response. Am J Med Genet B Neuropsychiatr Genet 174:427–434.
38. Bremner JD, Vermetten E (2004): Neuroanatomical changes associated with pharmacotherapy in posttraumatic stress disorder. Ann N Y Acad Sci 1032:154–157.
39. Vermetten E, Vythilingam M, Southwick SM, Charney DS, Bremner JD (2003): Long-term treatment with paroxetine increases verbal declarative memory and hippocampal volume in posttraumatic stress disorder. Biol Psychiatry 54:693–702.
40. Yang Z, Oathes DJ, Linn KA, Bruce SE, Satterthwaite TD, Cook PA, *et al.* (2018): Cognitive behavioral therapy is associated with enhanced cognitive control network activity in major depression and posttraumatic stress disorder. Biol Psychiatry Cogn Neurosci Neuroimaging 3:311–319.
41. MacNamara A, Rabinak CA, Kennedy AE, Fitzgerald DA, Liberzon I, Stein MB, *et al.* (2016): Emotion regulatory brain function and SSRI treatment in PTSD: Neural correlates and predictors of change. Neuropsychopharmacology 41:611–618.
42. Fonzo GA, Goodkind MS, Oathes DJ, Zaiko YV, Harvey M, Peng KK, *et al.* (2017): Selective effects of psychotherapy on frontopolar cortical function in PTSD. Am J Psychiatry 174:1175–1184.
43. Teicher MH, Samson JA (2016): Annual Research Review: Enduring neurobiological effects of childhood abuse and neglect. J Child Psychol Psychiatry 57:241–266.